Experimental study of isotherms and kinetics for adsorption of water on Aluminium Fumarate

Teo, How Wei Benjamin; Chakraborty, Anutosh; Kitagawa, Yuji; Kayal, Sibnath

2017

Teo, H. W. B., Chakraborty, A., Kitagawa, Y., & Kayal, S. (2017). Experimental study of isotherms and kinetics for adsorption of water on Aluminium Fumarate. International Journal of Heat and Mass Transfer, 114, 621-627.

https://hdl.handle.net/10356/86294

https://doi.org/10.1016/j.ijheatmasstransfer.2017.06.086

Experimental Study of Isotherms and Kinetics for Adsorption of water on Aluminium Fumarate

How Wei Benjamin, Teo[1], Anutosh Chakraborty[1,*], Yuji, Kitagawa[1,2], Sibnath Kayal[1]

[1]School of Mechanical and Aerospace Engineering, Nanyang Technological University, 50 Nanyang Avenue, Singapore 639798, Republic of Singapore

[2]School of Engineering, Tokyo Institute of Technology, Ookayama Campus, 2-12-1 Ookayama, Meguro-ku, Tokyo 152-8550, Japan

*Author to whom correspondence should be addressed, E-mail: AChakraborty@ntu.edu.sg

Abstract

This article presents the adsorption characteristics of Aluminium Fumarate (Al-Fum) Metal Organic Framework (MOF) and water systems for the temperatures ranging from 25°C to 60°C and pressures up to saturation conditions. The amount of water uptakes is measured by a gravimetric analyser under static and dynamic conditions. The surface characteristics of Al-Fum are performed by scanning electron microscopy (SEM), X-ray diffraction (XRD) and N_2 adsorption analysis. The experimentally measured water uptake data are fitted with Langmurian type isotherm and kinetic equations. The isosteric heat of adsorption is calculated from the concepts of pressure – temperature – uptake co-ordinate system. The pore size distribution shows a wide distribution of micropores. A decent 'S' – shaped isotherm curve is observed from the experimental results. Based on the isotherms and kinetics data, Al-Fum MOF shows a potential adsorbent for heat transmission applications such as heat pump and desalination.

Keywords: Adsorption isotherms, Adsorbent characteristics, Isosteric heat of adsorption, Kinetics, Aluminium Fumarate MOF, Water Adsorption

Introduction

The production of heating, cooling and fresh water employing low grade heat is essential from economic and environmental viewpoints, as the conventional vapour compression systems have already placed an escalating threat towards global warming and ozone depletion potentials. Therefore, adsorption assisted heat transmission process is necessary. Adsorption system is generally operated by solar radiation or waste heat generated from a cogeneration plant. The thermal compression (TC) is occurred in the adsorption bed during the adsorption and desorption of refrigerant. For adsorption assisted cooling, heating and desalination process, water is usually preferred to be the adsorbate as it is non-toxic, easily available and has high latent heat of evaporation [1]. The adsorbents are required to be mainly micro porous with higher pore volume and heterogeneous in nature. Currently, the adsorbents used for cooling, heat pump and desalination are silica gels and zeolites [2-7].

The major drawback of adsorption system is the bulky size of the system, which is mainly caused by the lower uptake difference (Δq) during the TC of an adsorption cycle. The lower working capacity of porous adsorbent available, from one adsorption cycle, is only a small part of the limiting water vapour uptakes. Hence, a large amount of adsorbent is needed to be installed in the test bed for sorption purposes [7]. The amount of adsorbate uptake on porous adsorbent relies upon the interaction between adsorbent – adsorbate systems and the pore structure of porous adsorbent [8, 9].

Currently, Metal Organic Frameworks (MOFs) has been attracted for adsorption assisted heat transmission applications due to their designable and high micro-porosity properties. These materials are made by the self-assembly of organic ligands and metal-containing nodes [10-14]. Recently, an aluminium based MOF, known as Aluminium Fumarate (Al-Fum), was synthesized

and patented by Kiener et al. [15]. The water adsorption capability on Al-Fum is high at relatively higher pressures.

Alvarez et al. [16] had compared the characteristics of Al-Fum with MIL-53(Al) by experimenting its selectivity with ethanol. Jeremias et al. [17] had synthesized Al-Fum adsorbents with additional coating for higher stability and thermal conductivity. Elsayed et al. [18] compared the water adsorption capability of Al-Fum with CPO-27(Ni) at 25°C under static and dynamic conditions. Both materials were found suitable for adsorption heat pump and desalination applications from simulation viewpoints.

In this paper, the synthesis process of the patented Al-Fum [15] is modified. The porous properties are characterised by SEM, XRD and N_2 adsorption isotherm analysis. To observe the amount of water uptake on Al-Fum MOF, water adsorption experiment is conducted by a gravimetric method for temperatures ranging from 25°C to 60°C and pressures up to the saturated region. The amount of water uptakes is also presented in time domain. The experimentally measured isotherms and kinetics data are fitted with the equations derived from the concept of Langmuir analogy [19, 20] within acceptable error ranges (< 5%). The isosteric heat of adsorption will be presented as a function of uptake employing Clausius – Clapeyron relation for the temperatures varying from 25°C to 60°C.

Experimental Setup

Synthesis

The synthesis of Al-Fum was performed at ambient pressure condition. First, 2.45g of aluminium chloride hexahydrate ($AlCl_3 \cdot 6H_2O$, Sigma-Aldrich) and 1.4g of fumaric acid ($C_4H_4O_4$, 99%) were added into the suspension of N, N-dimethylformamide (DMF, 99.8%,

50ml) in a beaker. Next, the suspension is stirred at 130°C for 4 days. After 4 days, the separation of the mixture is carried out using a centrifugal spinning machine. After separation, the white synthesized material is rinsed twice with acetone and methanol. Then, the synthesized material is heated at 80°C for drying. At last, the synthesized, powdered material is placed in the vacuum oven for 3 hours and heated at 150°C for activation.

Characterisation

XRD (X-ray diffraction) measurement (Shimadzu XRD-6000 diffractometer) were conducted with a step size of 0.02° using a monochromatic CuK_{α} radiation (wavelength = 0.154nm) operated at 40kV and 40mA. The microstructure, morphologies and particle size of the sample were determined by JEOL FESEM (Field Emission Scanning Electron Microscopy) operated at 5kV. The pore volume, pore size and specific surface area of Al-Fum were measured by N_2 adsorption/desorption isotherms data at 77K. The sample was heated at 160°C for 3 hours to remove all gas molecules before N_2 adsorption measurement. The isotherm results are equipped with BET (Brunuer-Emmet-Teller) equation to calculate BET surface area. The total pore volume is obtained by N_2 adsorption data under saturation conditions. If the isotherm is nearly horizontal throughout the range of P/P_s as it approaches to saturation, macro pores are not found in the adsorbent structure. Hence, the pore volume is defined properly. With the existence of macropores, the isotherm will have a sharp increase as P/P_s approaches to 1. The limiting uptake of the isotherm is used to identify as the total pore volume of adsorbent. Since N_2 is saturated at P/P_s = 1, the total pore volume is equivalent to the volume of liquid N_2 (V_{liq}) adsorbed in the adsorbent, and it is calculated by $V_{liq} = \frac{P_a V_{ads} V_m}{RT}$, where V_{ads} is the volume of N_2 adsorbed, V_m is the molar volume of liquid N_2 (3.47 x 10^{-5} m^3/mol), P_a and T are ambient

pressure and temperature, respectively. Using the known total pore volume and surface area, the average pore size (r_p) can be estimated by $r_p = \frac{2V_{liq}}{A_s}$, where S_{BET} is the BET surface area.

Water Adsorption

The amount of water vapour on Al-Fum MOF at different temperatures and pressures are measured by a thermogravimetric analyser (TGA) due to the high accuracy and ease of control of pressure and temperature during experimentation. The TGA contains two microbalances with a maximum load capacity of 5 g ± 0.1 μg each, which is housed in a temperature-controlled chamber (200 cm^3). Hence the microbalance measures the mass gain, or loss, over time. The TGA gives a direct measurement of the adsorbate uptake throughout the adsorption process. A microbalance is used to measure the adsorbate mass as a function of humidity ratio or relative pressure (P/P_s) and time for a given temperature, T. The scheme of the TGA apparatus is shown in Figure 1. In the TGA, the adsorbent container is suspended on an extension wire. The wire is connected to the microbalance. The water vapour is generated in a humidifier (shown in Figure 1). The temperature inside the humidifier is measured by a class A RTD temperature sensor with an accuracy of ± 0.15 ^oC. The vapour charging flow rate is controlled automatically by a control panel. A vacuum pump is used for vacuuming and purging the system before an experiment and maintaining the adsorption chamber pressure in coordination with a vacuum controller. The micro-balance measures the mass of adsorbent sample and it can detect the change of water vapour mass within the sample in a very short time. A small furnace is used to provide isothermal environment on the adsorbent container whilst a temperature sensor measures the temperature of the chamber. The water vapour pressure is detected by the humidity sensor.

The dry mass of Al-Fum is obtained via heating at 120°C for two hours in an oven before isotherms and kinetics experiment. Al-Fum adsorbent is then placed on the sample cell of the analyser, which is held by a microbalance located at the top of the Adsorption Chamber. For this experimental set up, the isothermal environment surrounding of the Al-Fum is required to be maintained by direct heating. The heaters are placed at the door and around the hermetic reaction chamber and homogenized by cooling air through the chamber and radiant heater. The dry Al-Fum MOF is maintained inside the adsorption chamber by direct radiant heating of 90°C with continuous supply of dry nitrogen (99.999% purity) to remove all moisture from the sample. The system performs the isotherms measurement once the regeneration process is completed. To prevent any condensation effects, the temperatures of adsorption chamber are required to set at least 15°C above the experimental conditions. Dry Nitrogen will be introduced continuously to the adsorption chamber to control the buoyancy effect of the microbalance.

During the adsorption experiment, the pressure and temperature of the adsorption chamber are measured within acceptable error ranges. The humidity probe stabilises the value of relative pressure (P/P_s) in the adsorption chamber by regulating the flow rate of dry N_2. If P/P_s is higher than that of expected values, the flow rates of dry N_2 are increased and the N_2 flow across the humidifier is halted. The excess water vapour is purged out of the chamber so that the P/P_s can be achieved at the desired value, which also introduces the right distribution of dry nitrogen to water vapour. If P/P_s is lower, the dry N_2 flow through the humidifier is increased for the addition of water vapour content within the adsorption chamber. The water vapour uptake is measured by the known values of P/P_s for a given temperature. During the adsorption process, the overall sample mass in terms of pressure, $M_s\,(P_i)$, is increased due to the addition of water vapour from the humidifier. Hence, the mass of adsorbate, m_a, is measured by $m_{a,i} = M_s(P_i) -$

$M_s(P_0)$, where i is the variable that signifies each pressure point, and $M_s\,(P_o)$ is the mass of Al-Fum + water vapour at initial known pressure of P_o. The gravimetric water uptake is calculated by $q_i = m_{a,i}/M_s$ for each pressure point, where M_s is the mass of dry solid adsorbent. The change in mass (final reading – initial reading) of Al-Fum – water system due to the increase of water vapour uptake is measured with respect to time, and these mass changes are varied from the transient to steady states at different pressure points. Thus, the gravimetric method enables a handful of adsorption uptake data to be taken under static and dynamic conditions. Employing the same method, the water adsorption measurement on Al-Fum is repeated at least three times to ensure that the repeatability is achieved within experimental uncertainties. The data related to the increase in pressure (P) with respect to temperature (T) are captured during experimentation. A plot of ln (P) versus (1/T) extracts the isosteric heats of adsorption for any water vapour uptake. All experimental data produce straight lines with higher regression coefficients. The slopes determine the value of $-Q_{st}/R$, where Q_{st} indicates the isosteric heat of adsorption and R is the gas constant.

Isotherm and Kinetics Modelling

The experimentally measured water vapour uptake on Al-Fum under static and dynamic conditions are fitted with adsorption isotherms and kinetics models. The theoretical models are generally utilized to understand adsorbent – adsorbate behaviour in a pressure – temperature – uptake coordinate system. From the experimental data, it is found that Al-Fum + water system indicates 'S'-shaped isotherm curves. For simplicity, the 'S'-shaped isotherm model is given by [19]

$$\theta = \frac{K(P/P_S)^m}{1+(K-1)(P/P_S)^m} \qquad (1)$$

where $K = \alpha exp\left[m(Q_{st}^{*} - h_{fg})/RT\right]$, α is the pre-exponential coefficient, m defines the heterogeneity factor, Q_{st}^{*} is the isosteric heat of adsorption at zero surface coverage, h_{fg} defines the enthalpy of evaporation and R is the gas constant. θ is the adsorbate coverage and is given by q/q^{o}, where q is the amount of water vapour uptake as a function of pressure and temperature, and q^{o} indicates the limiting uptake. It is also known that $\left(Q_{st}^{*} - h_{fg}\right)$ is featured as the adsorption characteristics energy [20] and can also be approximated from experimental data.

Employing the concept of Langmurian analogy, the adsorption equilibrium constant K is expressed in terms of adsorption and desorption rate coefficients k_{ads} and k_{des}, respectively i.e. $K = k_{ads}/k_{des}$. Using the value of K from equation (1), the adsorption surface coverage (θ) under equilibrium conditions becomes [20]:

$$k_{des}\theta[1 - (P/P_s)^m] = k_{ads}(1 - \theta)(P/P_s)^m. \quad (2)$$

According to Langmuir, adsorption is regarded as a reversible process between adsorbent and adsorbate molecules [21, 22]. Therefore, under non-equilibrium condition, the amount of adsorbate surface coverage as a function of time (θ_t) is expressed as [23]

$$\frac{\mathrm{d}\theta_t}{\mathrm{d}t} = k_{ads}(1 - \theta_t)\left(\frac{P}{P_s}\right)^m - k_{des}\theta_t\left[1 - \left(\frac{P}{P_s}\right)^m\right] \quad (3)$$

With the relation between k_{ads} and the gas molecular collision frequency, the adsorption coefficient, k_{ads}, is calculated as $k_{ads} = W\beta A_s$, where W is the number of collisions of molecules with the surface per unit time, A_s is the specific surface area of the adsorbent and β is shown as the sticking coefficient. The number of collisions of molecules with adsorbent surface is determined by $W = MP/\sqrt{2\pi MRT}$, where M is the molecular weight of molecules in *gram* per *mole*. The sticking coefficient is determined by $\beta = [\beta_0 \exp(-E_a/RT)]$, where β_o is the pre-

exponential or frequency factor and E_a is the activation energy [24]. Rearranging Equation (3), the first order equation can be written as

$$\frac{\mathrm{d}\theta_t}{\mathrm{d}t} = k_{ads}\left(\frac{P}{P_s}\right)^m - \theta_t\left\{k_{ads}\left(\frac{P}{P_s}\right)^m + k_{des}\theta_t\left[1-\left(\frac{P}{P_s}\right)^m\right]\right\}$$

$$= k_{ads}\left(\frac{P}{P_s}\right)^m - \theta_t\frac{1}{\tau} \quad (4)$$

where $1/\tau = k_{ads}(P/P_s)^m + k_{des}\theta_t[1-(P/P_s)^m]$ is the time constant [20]. After achieving the analytical solution of Equation (4), the equation is written as $\theta_t = C'e^{\frac{-t}{\tau}} + (k_{ads}(P/P_s)^m)/(1/\tau) = C'e^{\frac{-t}{\tau}} + \theta$. Using the initial condition ($\theta = \theta_{ini}$ at $t = 0$) of the adsorption process, the constant $C'$is found to be $\theta_{ini} - \theta$. Thus, with rearrangement [20], the kinetic theoretical model is written as

$$\theta_t = \theta - \theta e^{\frac{-t}{\tau}} + \theta_{ini}e^{\frac{-t}{\tau}} \rightarrow \theta_t - \theta_{ini} = \theta - \theta e^{\frac{-t}{\tau}} + \theta_{ini}e^{\frac{-t}{\tau}} - \theta_{ini}$$

$$\theta_t - \theta_{ini} = \theta\left(1-e^{\frac{-t}{\tau}}\right) - \theta_{ini}\left(1-e^{\frac{-t}{\tau}}\right)$$

$$\frac{\Delta\theta_t}{\Delta\theta} = \frac{\theta_t-\theta_{ini}}{\theta-\theta_{ini}} = 1-e^{\frac{-t}{\tau}} \quad (5)$$

Equation (5) has also been shown by the works of Aristov et al. [25].

Results and Discussion

Characterisation

Figure 2 shows the SEM (Scanning Electro-Microscopy) diagram for the Al-Fum. The size of the sample is about 1μm with quadrahedral shape. The shape synchronises with the molecular structure of Al-Fum [16, 26]. Hence, this proves that Al-Fum is synthesized correctly. It is noted the particles have a strong agglomeration, which is very similar to MOF801 [27]. Figure 3 shows

the PXRD (Powder X-Ray Diffraction) graphs of the Al-Fum. The first peak can be seen at 10 degree with small peaks shown at higher angles. The peaks correlate the intensity of Al^{3+} in the adsorbent structure. It also shows that the purification of the material was properly done. Thus, the material structure is stable as no additional peaks are detected.

Figure 4 shows the N_2 adsorption isotherm on Al-Fum adsorbent. From the experimental data, it is found that the volumetric N_2 uptake for Al-Fum is within 300 to 400 cm^3/cm^3 of adsorbent before approaching to saturated pressure. As approaching towards the saturated pressure, the volumetric uptake increases up to approximately 1400 cm^3/cm^3 of sorbent. This suggests that the material has large variations of micropores and macropores within Al-Fum structure. The pore width, pore volume and surface area are calculated employing BET analysis and N_2 adsorption data. These data are furnished in Table 1. For comparison purposes, the pore width, volume and specific surface area of MIL-101(Cr) MOF and AQSOA-Z05 zeolite are also shown in Table 1. With the comparison of previous work, Al-Fum has lower BET surface area and pore volume as compared to MIL-101(Cr). Nonetheless, the average pore size of Al-Fum is smaller as compared to that of MIL-101(Cr). This is due to the lack of benzene chemical structure of fumaric acid used to synthesized Al-Fum. Further comparison was made with AQSOA-Z05, and it shows that Al-Fum has higher BET surface area and pore volume. The average pore size of Al-Fum is also shown to be smaller than that of AQSOA-Z05. This may be possible as C atoms are smaller than P atoms. Figure 5 shows the Pore Size distribution of Al-Fum. The smallest pores are estimated to have a width of 6Å. Subsequently, the next two peaks are estimated with a width of 7Å and 11Å. Thus, Figure 5 shows that Aluminium Fumarate consists majority of micropores throughout its surface.

Water Adsorption Isotherms

Figure 6 shows the adsorption – desorption phenomena of Al-Fum + water system. Hence, for Al-Fum + water and AQSOA-Z05 + water systems [28, 29], the uptakes are measured in the direction of adsorption as the amount of water vapor uptake is increased with pressure. When the equilibrium is achieved at the maximum uptake point, the system is depressurized and the uptakes ate measured and recorded in the direction of desorption. In the present experiment the adsorption–desorption cycle is repeated at least two times to establish the repeatability of experimental data. A hysteresis behaviour in the adsorption-desorption curve is observed at very low pressures. This occurs due to the fact that desorption process is not completed. Some residual water remains trapped in the porous adsorbents even when the pressure is low. It is also found from Figure 6 that the adsorption uptake increases greatly for the relative pressure above $P/P_s \geq 0.2$. Subsequently, the uptake increases in a gentle slope for the relative pressure of $P/P_s \leq 0.3$. As it approaches to saturated pressure, a slight increase of uptake is observed due to the existence of marcopores. It is also noted that the desorption isotherm for Al-Fum has almost the same trend as its adsorption behaviour. The highest uptake – offtake difference between the adsorption and desorption isotherm of Al-Fum is $\Delta q = 0.12$. For comparison purposes, the adsorption isotherms of AQSOA-Z05 are also shown in Figure 6. The comparison is performed as both materials contain Al^{3+} metal nodes in its structure. Based on the isotherms, AQSOA-Z05 has longer hydrophobic length ($0 \leq P/P_s \leq 0.25$) as compared with Al-Fum. It is also shown that Al-Fum ($q = 0.37$ at $P/P_s = 0.35$) has higher uptake as compared to AQSOA-Z05 ($q = 0.2$ at $P/P_s = 0.35$). Since AQSOA-Z05 consists of AlO_4 and PO_4 structure, this may form lesser micropores to initiate water adsorption at a lower pressure. On the other hand, Al-Fum mainly consists of Al, C and O atoms. This may indicate that having carbon atoms in solid adsorbent allows better pore size distribution for water adsorption process.

The experimentally measured isotherm data of Al-Fum + water system for temperatures ranging from 25°C to 60°C and pressures up to saturated regions are shown in Figure 7. Employing the isotherm model (Equation 1), the experimental results are fitted for type V isotherm curves within an acceptable range of 5%. The isotherm parameters such as the heterogeneity factor (m), the isosteric heat of adsorption at zero surface coverage (Q_{st}^{*}), pre-exponential coefficient (α) and the limiting uptake (q^{o}) are shown in Table 2. It is noted that α relates to the entropy of adsorption and m is responsible to the shape of isotherm curve.

Water Adsorption Kinetics

Figure 8 shows the water uptake of Al-Fum at 25°C and 60°C as a function of time. The adsorption rate at 25°C is much longer than that of 60°C as the dynamic conditions is measured at two different pressures. The kinetics model (Equation 5) is fitted with the experimentally measured data within acceptable error range of 5%. Employing the Langmuir constant, K, estimated from Equation 1 and surface area, the adsorption kinetic constant of k_{ads} can be determined, which is shown in Table 3. The activation energy, E_a, for Al-Fum is also presented in Table 3. The frequency factor, β_o, is considered as 1 since a thin layer of adsorbent [20] is used for the experiment. Based on these results, longer cycle time is required to implement Al-Fum as adsorbent for adsorption chiller or heat pumps.

Isosteric Heat of Adsorption

Figure 9 shows the isosteric heat of adsorption (Q_{st}) of Al-Fum + water systems based on Clausius – Clapeyron relation for the temperatures varying from 25°C to 60°C. A sharp increase of Q_{st} is observed at the Henry's or low uptake region, follow by a gentle increment of energy as uptake increases. This is due to the fact that at the beginning of adsorption, the water molecules are adsorbed rapidly onto sites of higher energy initially. In the second stage, the interaction

between Al-Fum and water molecule is continued to increase due to the presence of micro-porosity in Al-Fum structure. Finally, a sharp decrement of Q_{st} is observed at the saturated pressure region as meso and macro pores are available in the material structure. Therefore, water molecules are adsorbed at low energy sites at limiting uptake region.

Conclusions

Al-Fum was synthesized and the porous properties are characterised for water adsorption experiment. The static and dynamic behaviours of Al-Fum + water system is experimentally measured by gravimetric method. From experimental data, a decent hydrophobic length of water uptake is observed. It is also noted that the adsorption and desorption isotherms at 25°C provide the similar trends. The isotherms and kinetics equations are fitted with experimentally measured data within the acceptable range of 5%. Hence, it is also found that the adsorption isotherm coefficients ($K = k_{ads}/k_{des}$) calculating from the isotherm model are used to estimate the adsorption (k_{ads}) and desorption (k_{des}) rate coefficients. The isosteric heat of adsorption is approximated from experimental isotherms in a pressure-temperature-uptake coordinate system. This study provides detailed experimental and theoretical findings of Al-Fum for water adsorption process. By analysing experimental data, we find that to replace Al-Fum from the current conventional adsorbents, these theoretical parameters of Al-Fum + water system are useful for designing an adsorption assisted heat transmission application.

Nomenclature

S_{BET}	BET surface area,	m^2/kg
E_a	activation energy,	J/mol

h_{fg}	latent heat of vaporisation	kJ/kg
K	Langmuir coefficient	
k_{ads}	adsorption rate coefficient	g/g s^{-1}
k_{des}	desorption rate coefficient	g/g s^{-1}
m	heterogeneity parameter	
P	pressure	kPa
P_s	saturated pressure	kPa
P_a	ambient pressure	
q	amount of water vapour uptake	
q^o	limiting uptake	
Q_{st}	isosteric heat of adsorption	kJ/kg
Q_{st}^*	isosteric heat of adsorption in Henry's region	kJ/kg
r_p	average pore size	Å
R	gas constant	
T	temperature	K
t	time	s
v_p	pore volume	cm^3/g
V_{liq}	volume of liquid N_2	m^3
V_{ads}	volume of N_2 adsorbed	m^3
V_m	molar volume of liquid N_2, 3.47 x 10^{-5}	m^3/mol

Symbol

α	pre-exponential coefficient (isotherm model)
β	sticking coefficient

β_o	pre-exponential coefficient (sticking coefficient)
τ	time constant, s
θ	adsorption uptake fraction
θ_{ini}	initial adsorption uptake fraction
θ_t	real time adsorption uptake fraction

Acknowledgements

The authors acknowledge the financing support from Ministry of Education (MOE), Singapore (grant no. MOE 2014-T2-2-061).

References

[1] Ali, S. M., Chakraborty, A., Adsorption assisted double stage cooling and desalination employing silica gel + water and AQSOA-Z02 + water systems, *Energy Conversion and Management*, vol. 117, pp. 193-205, 2016.

[2] Saha, B.B., Akisawa, A., Kashiwagi, T. Solar/waste heat driven two-stage adsorption chiller: The prototype, *Renewable Energy*, vol. 23, pp. 93-101, 2001.

[3] Zhang, G., Wang, D.C., Zhang, J.P., Han, Y.P., Sun, W., Simulation of operating characteristics of the silica gel-water adsorption chiller powered by solar energy, *Solar Energy*, Vol. 85, pp. 1469-1478, 2011.

[4] Radu, A.I., Defraeye, T., Ruch, P., Carmeliet, J., Derome, D., Insights from modeling dynamics of water sorption in spherical particles for adsorption heat pumps, *International Journal of Heat and Mass Transfer*. Vol. 105, pp. 326-337, 2017.

[5] Saha, B. B., Akisawa, A., and Kashiwagi, T., Silica gel water advanced adsorption refrigeration cycle, *Energy,* vol. 22, pp. 437-447, 1997.

[6] Wang, L. W., Wang, R. Z., and Oliveira, R. G., A review on adsorption working pairs for refrigeration, *Renewable and Sustainable Energy Reviews,* vol. 13, pp. 518-534, 2009.

[7] Thu, K., Yanagi, H., Saha, B.B., Ng, K.C., Performance investigation on a 4-bed adsorption desalination cycle with internal heat recovery scheme, *Desalination,* vol. 1402, pp. 88-96, 2017.

[8] Furukawa, H., Gandara, F., Zhang, Y. B., Jiang, J., Queen, W. L., Hudson, M. R., and Yaghi, O. M., Water adsorption in porous metal-organic frameworks and related materials, *J Am Chem Soc,* vol. 136, pp. 4369-81, Mar 19 2014.

[9] Teo, H. W. B., Chakraborty, A., and Ooi, K. T., Adsorption Characteristics of Modified MIL-101(Cr) for Gas (Mainly CH_4) Storage Applications, presented at the ASME International Mechanical Engineering Congress and Exposition, Houston, Texas, USA, 2015.

[10] Chui, S. S. Y., Lo, S. M. F., Charmant, J. P. H., Orpen, A. G., and Williams, I. D., A Chemically Functionalizable Nanoporous Material [Cu3(TMA)2(H2O)3]n, *Science,* vol. 283, pp. 1148-1150, 1999.

[11] Ferey, G., Mellot-Draznieks, C., Serre, C., Millange, F., Dutour, J., Surble, S., and Margiolaki, I., A chromium terephthalate-based solid with unusually large pore volumes and surface area, *Science,* vol. 309, pp. 2040-2042, Sep 23 2005.

[12] Hong, D.-Y., Hwang, Y. K., Serre, C., Férey, G., and Chang, J.-S., Porous Chromium Terephthalate MIL-101 with Coordinatively Unsaturated Sites: Surface Functionalization,

Encapsulation, Sorption and Catalysis, *Advanced Functional Materials,* vol. 19, pp. 1537-1552, 2009.

[13] Kitagawa, S. and Uemura, K., Dynamic porous properties of coordination polymers inspired by hydrogen bonds, *Chem Soc Rev,* vol. 34, pp. 109-19, Feb 2005.

[14] Li, H., Mohamed Eddaoudi, O'Keeffe, M., and Yaghi, O. M., Design and synthesis of an exceptionally stable and highly porus Metal-Organic Framework, *Nature,* vol. 402, pp. 276 - 279, 1999.

[15] Kiener, C., Muller, U., and Schubert, M., Organometallic Aluminum Fumarate Backbone Material, USA Patent US20090092818A1, 2009.

[16] Alvarez, E., Guillou, N., Martineau, C., Bueken, B., Van de Voorde, B., Le Guillouzer, C., Fabry, P., Nouar, F., Taulelle, F., de Vos, D., Chang, J. S., Cho, K. H., Ramsahye, N., Devic, T., Daturi, M., Maurin, G., and Serre, C., The structure of the aluminum fumarate metal-organic framework A520, *Angew Chem Int Ed Engl,* vol. 54, pp. 3664-8, Mar 16 2015.

[17] Jeremias, F., Fröhlich, D., Janiak, C., and Henninger, S. K., Advancement of sorption-based heat transformation by a metal coating of highly-stable, hydrophilic aluminium fumarate MOF, *RSC Advances,* vol. 4, p. 24073, 2014.

[18] Elsayed, E., Al-Dadah, R., Mahmoud, S., Elsayed, A., and Anderson, P. A., Aluminium fumarate and CPO-27(Ni) MOFs: Characterization and thermodynamic analysis for adsorption heat pump applications, *Applied Thermal Engineering,* vol. 99, pp. 802-812, 2016.

[19] Sun, B. and Chakraborty, A., Thermodynamic formalism of water uptakes on solid porous adsorbents for adsorption cooling applications, *Applied Physics Letters*, vol. 104, p. 201901, 2014.

[20] Sun, B. and Chakraborty, A., Thermodynamic frameworks of adsorption kinetics modeling: Dynamic water uptakes on silica gel for adsorption cooling applications, *Energy,* vol. 84, pp. 296-302, 2015.

[21] Langmuir, I., The Adsorption of Gases on Plane Surfaces of Glass, Mica and Platinum, *Journal of the American Chemical Society,* vol. 40, pp. 1361-1403, 1918.

[22] Langmuir, I., The Evaporation, Condensation and Reflection of Molecules and the Mechanism of Adsorption, *Physical Review,* vol. 8, pp. 149-176, 1916.

[23] Liu, Y. and Shen, L., From Langmuir Kinetics to First- and Second-Order Rate Equations for Adsorption, *Langmuir,* vol. 24, pp. 11625-11630, 2008.

[24] Asnin, L. D., Chekryshkin, Y. S., and Fedorov, A. A., Calculation of the sticking coefficient in the case of the linear adsorption isotherm, *Russian Chemical Bulletin,* vol. 52, pp. 2747-2749, 2003.

[25] Aristov, Y. I., Glaznev, I. S., and Girnik, I. S., Optimization of adsorption dynamics in adsorptive chillers: Loose grains configuration, *Energy,* vol. 46, pp. 484-492, 2012.

[26] Henninger, S. K., Ernst, S.-J., Gordeeva, L., Bendix, P., Fröhlich, D., Grekova, A. D., Bonaccorsi, L., Aristov, Y., and Jaenchen, J., New materials for adsorption heat transformation and storage, *Renewable Energy,* Vol. 110, pp. 59-68, 2017.

[27] Wißmann, G., Schaate, A., Lilienthal, S., Bremer, I., Schneider, A. M., and Behrens, P., Modulated synthesis of Zr-fumarate MOF, *Microporous and Mesoporous Materials,* vol. 152, pp. 64-70, 2012.

[28] Teo, H. W. B., Chakraborty, A., and Fan, W., Improved adsorption characteristics data for AQSOA types zeolites and water systems under static and dynamic conditions, *Microporous and Mesoporous Materials*, vol. 242, pp. 109-117, 2017.

[29] Kayal, S., Sun, B., Saha, B.B. Adsorption characteristics of AQSOA zeolites and water for adsorption chillers, *International Journal of Heat and Mass Transfer*, vol. 92, pp. 1120-1127, 2016.

List of Figures

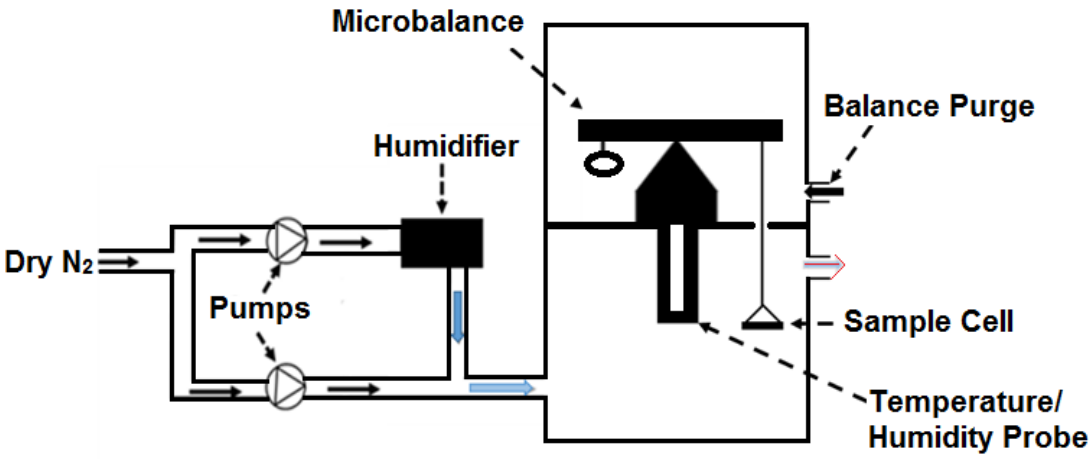
Microbalance
Balance Purge
Humidifier
Dry N_2
Pumps
Sample Cell
Temperature/
Humidity Probe

Figure 1

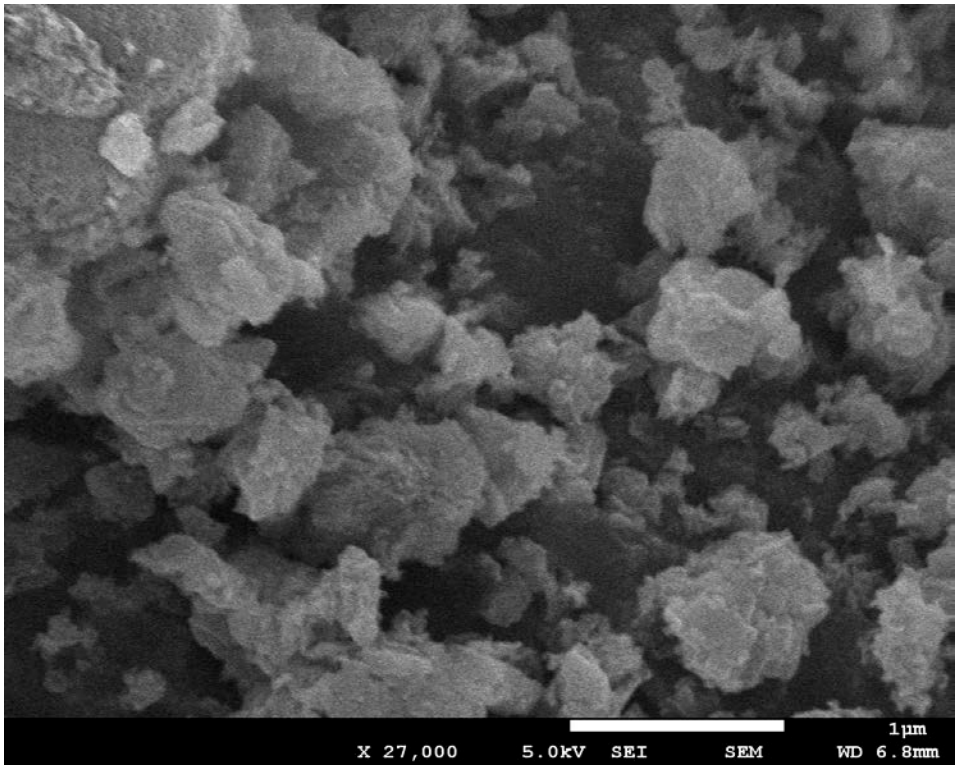

Figure 2

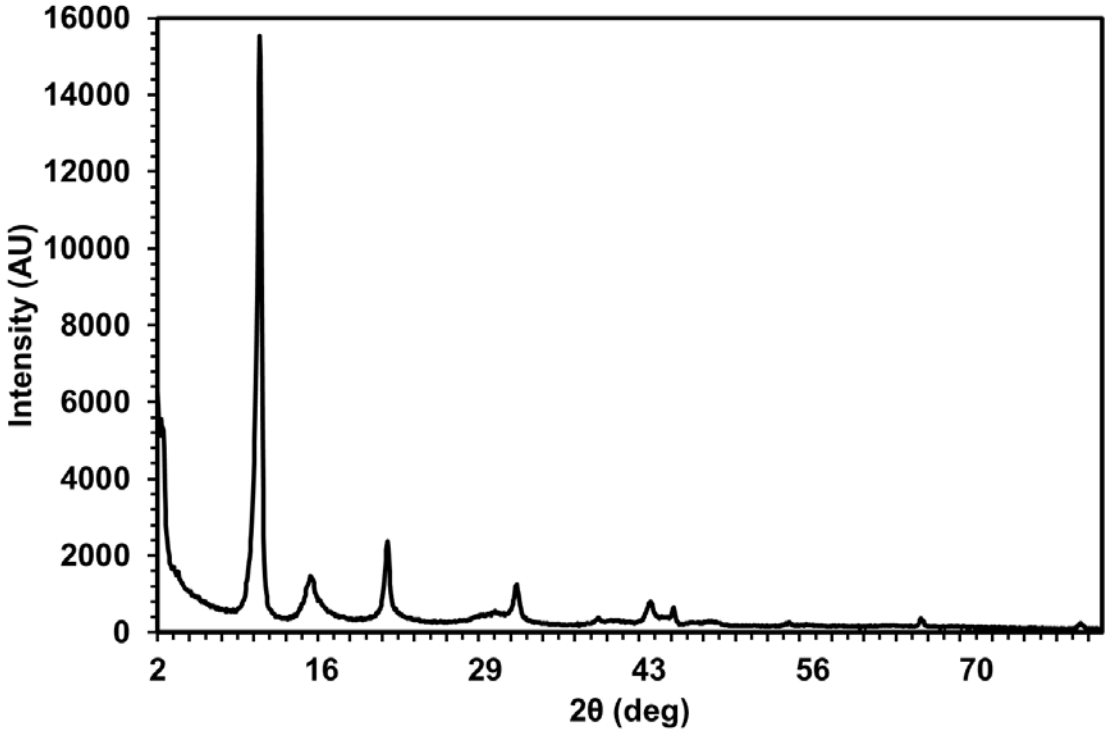
16000
14000
12000
10000
8000
6000
4000
2000
0
Intensity (AU)
2
16
29
43
56
70
2θ (deg)

Figure 3

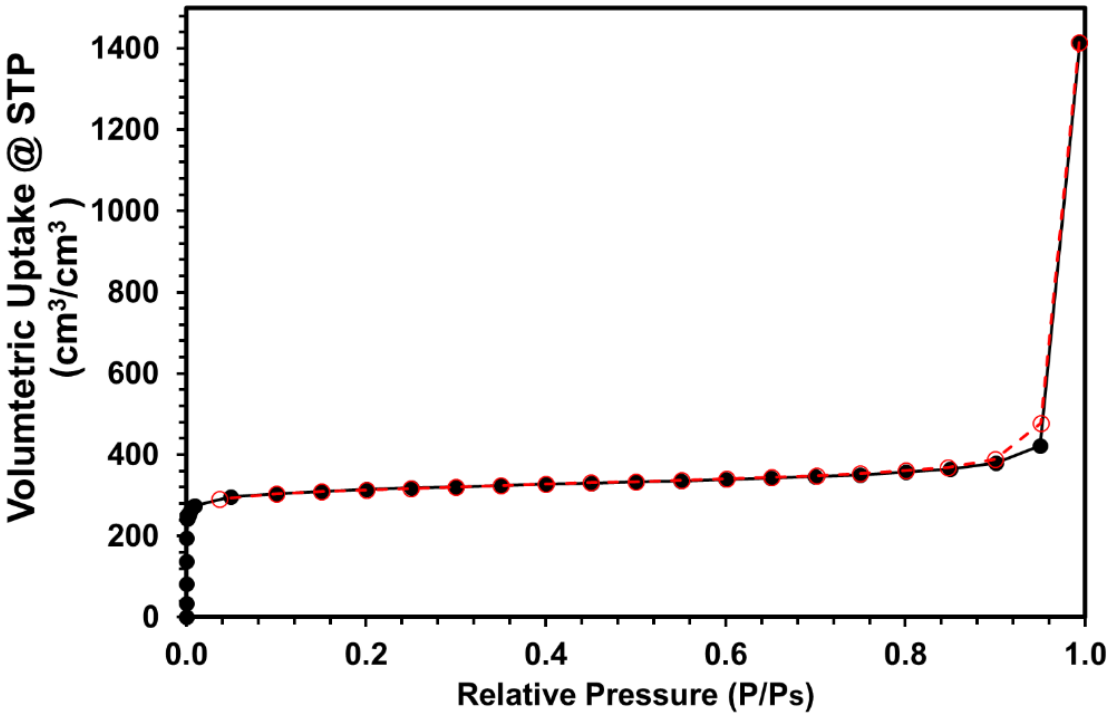
Volumtetric Uptake @ STP
(cm3/cm3)
1400
1200
1000
800
600
400
200
0
0.0
0.2
0.4
0.6
0.8
1.0
Relative Pressure (P/Ps)

Figure 4

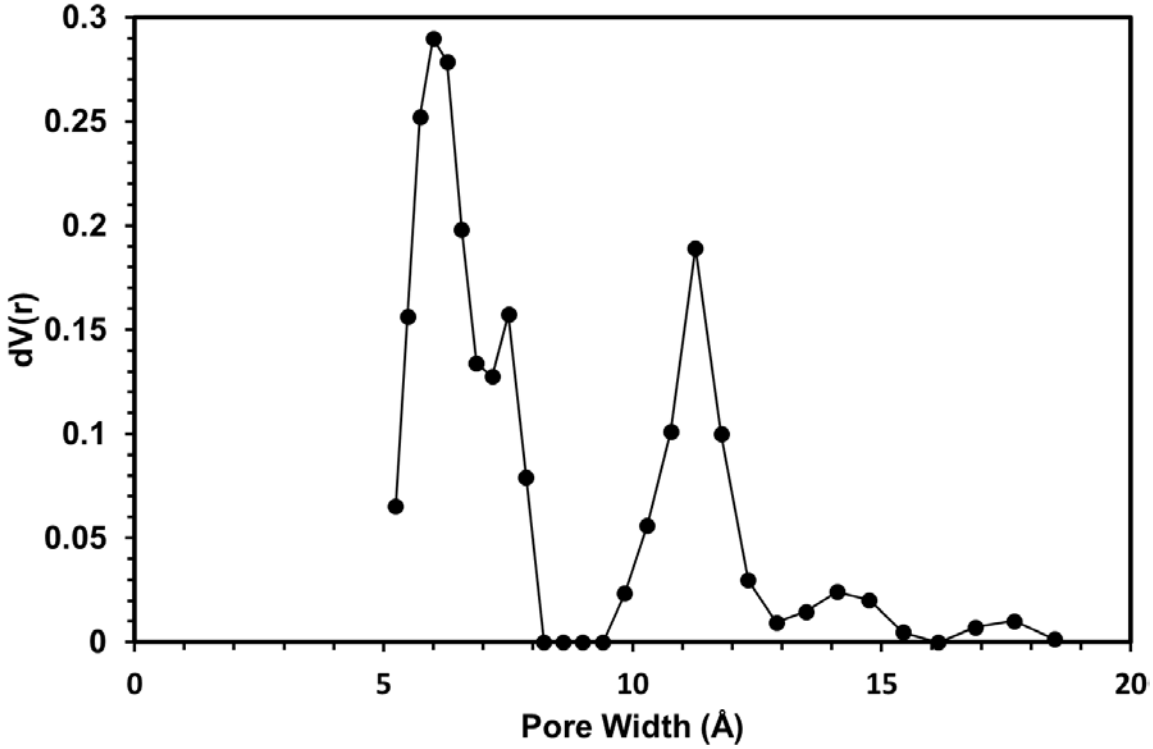

Figure 5

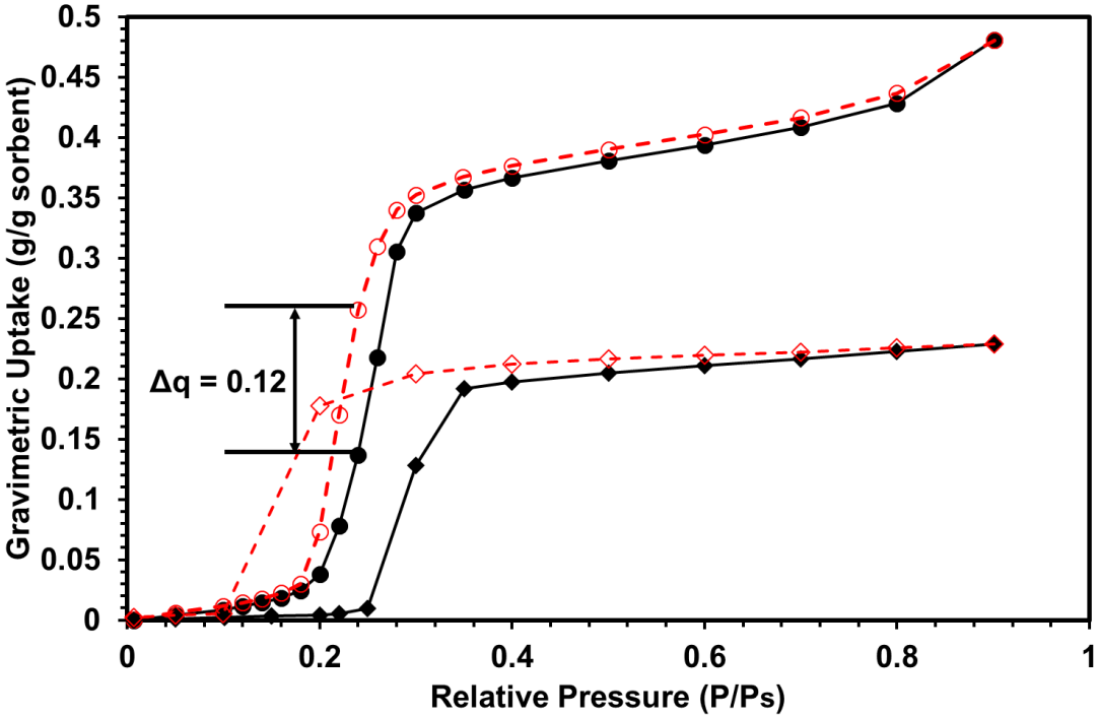
Gravimetric Uptake (g/g sorbent)
Relative Pressure (P/Ps)
Δq = 0.12
0
0.05
0.1
0.15
0.2
0.25
0.3
0.35
0.4
0.45
0.5
0
0.2
0.4
0.6
0.8
1

Figure 6

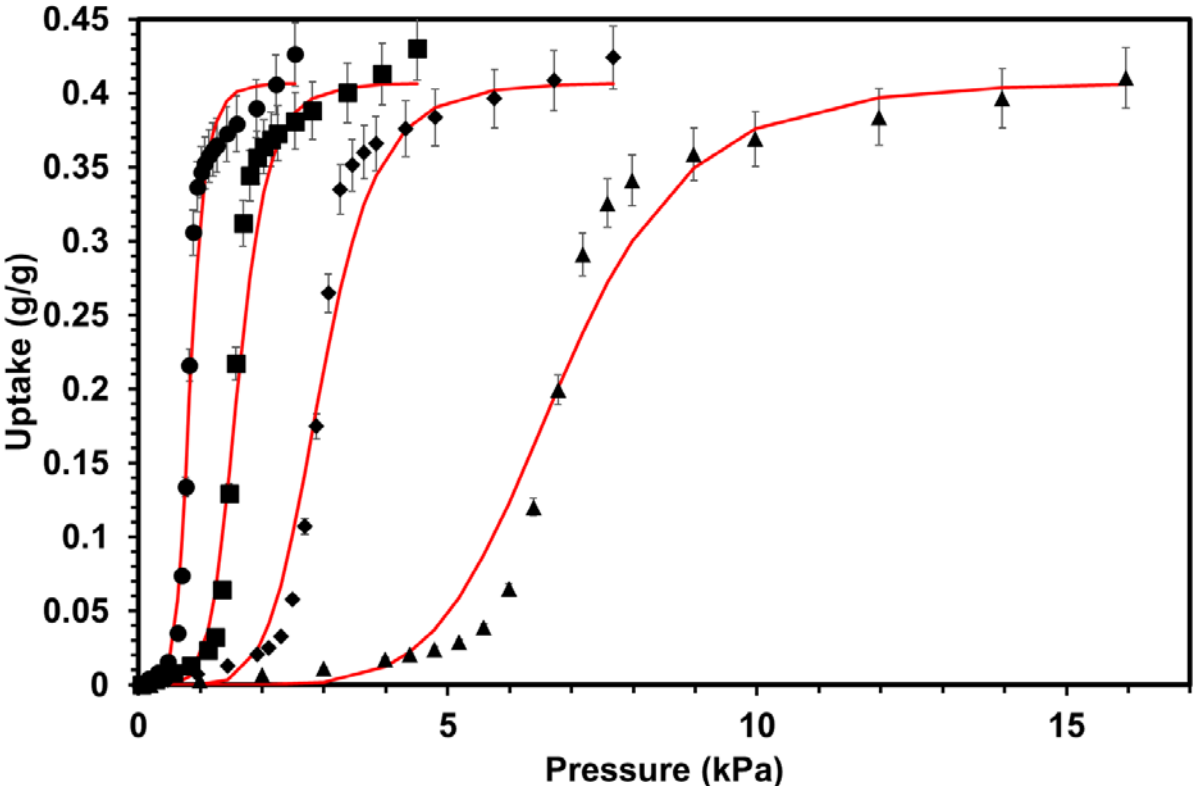

Figure 7

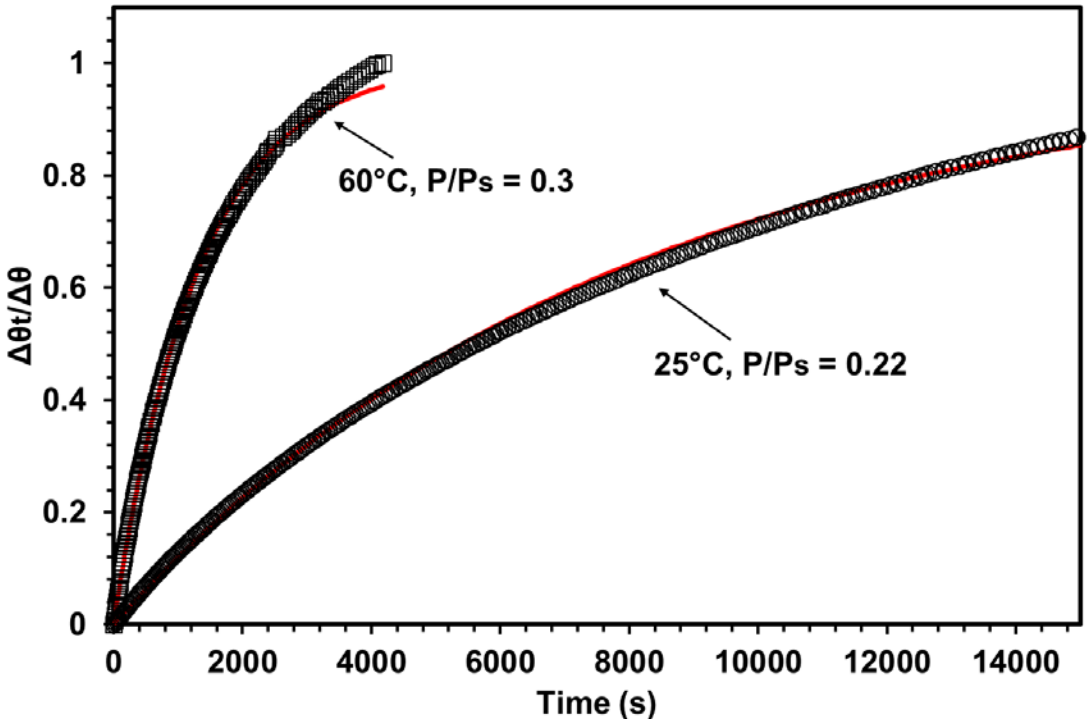
1
0.8
0.6
0.4
0.2
0
Δθt/Δθ
0
2000
4000
6000
8000
10000
12000
14000
Time (s)
60°C, P/Ps = 0.3
25°C, P/Ps = 0.22

Figure 8

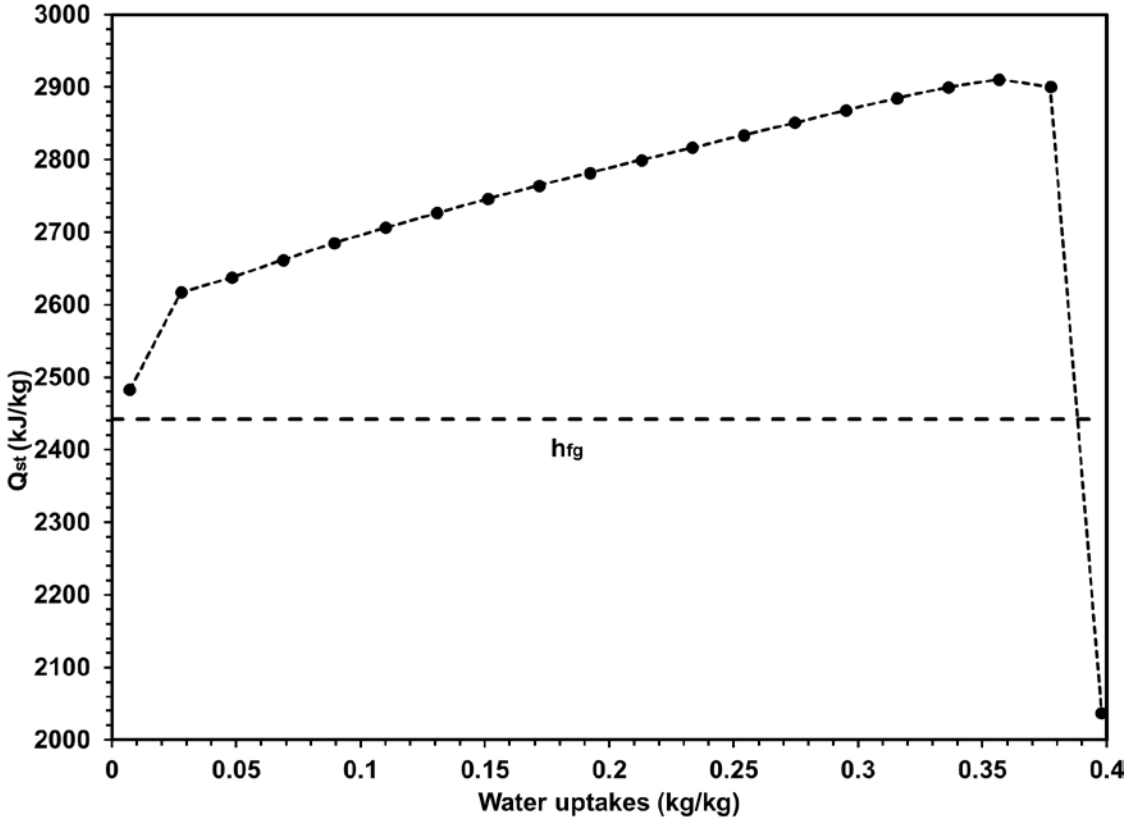
3000
2900
2800
2700
2600
2500
2400
2300
2200
2100
2000
Qst (kJ/kg)
hfg
0
0.05
0.1
0.15
0.2
0.25
0.3
0.35
0.4
Water uptakes (kg/kg)

Figure 9

Table 1: N_2 Adsorption Analysis

Adsorbent	BET Surface Area (m^2/g)	Pore Volume (cm^3/g)	Average Pore Radius (Å)	Ref
Al-Fum	792.26	0.926	10.91	This work
MIL-101	3402.69	1.597	11.3905	Previous Work
AQSOA-Z05	187.1	0.07	11.76	Previous work, [22]

Table 2: Parameters of proposed isotherm model for various MIL-101 + water systems

System	q^o (kg /kg)	Q_{st}^* (kJ/kg)	m	α
Al-Fum + Water	0.407	2780	6.5	6.78×10^{-4}

Table 3: Parameter of adsorption kinetics for Aluminium Fumarate + Water systems

System	k_{ads} (1/s)	β_o	E_a (J/mol)
Al-Fum + Water	$14705.93\left(\frac{\beta_o.P}{\sqrt{T}}\right)\exp\left(\frac{-E_a}{RT}\right)$	1	36660
$K = k_{ads}/k_{des}$. Hence the pressure P is in Pa and the temperature T is in K. The isotherm coefficient K is obtained from equation 1.			